Supplementary Information

Revolutionizing Lithium-Ion Batteries: Exploiting Liquid Crystal Electrolytes

Sijie Liu[1,2+], Le Zhou[3+], Yun Zheng[4*], Kristiaan Neyts[3*]*

[1] Research Institute of Tsinghua University in Shenzhen, Shenzhen, Guangdong 518000, P. R. China.

[2] Institute of Nuclear and New Energy Technology, Tsinghua University, Beijing, 100084, P. R. China.

[3] SKLADT, The Hong Kong University of Science and Technology, Clear Water Bay, Hong Kong, P. R. China.

[4] Institute of New Energy Materials and Engineering, College of Materials Science and Engineering, Fuzhou University, Fuzhou, 350108, P. R. China.

E-mail: liusijie@tsinghua.edu.cn; yunzheng@fzu.edu.cn; eeneyts@ust.hk

Table S1. Nanostructure dimensionality of LCEs

Phase Type	Ion Channel Dimension	Ionic Conductivity	Key Advantages
Cubic (3D)	3D interconnected	Highest (>10^{-3} S cm^{-1})	Isotropic ion transport; stable at low temperatures
Smectic (2D)	2D layered	Moderate (~10^{-4} S cm^{-1})	Anisotropic conduction; tunable layer spacings
Columnar (1D)	1D channel	Lowest (~10^{-5}-10^{-8} S cm^{-1})	Ease of alignment via external fields, temperature or surface

Table S2 The commercialization process of LCEs

Number	Chemical Formula	Ion Transport Mechanism	Ionic/Non-ionic	Ionic Conductivity (σ)	Remarks under Specific Conditions	Commercialization process	ref.
1.	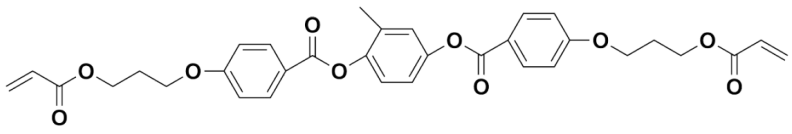	2D	non-ionic	$3 \pm 0.5 \times 10^{-3}$ S cm^{-1} at room temperature		RM257 is an industrial-grade UV liquid crystal monomer for LCEs, used in smart devices and lithium batteries. It dissolves easily, has low viscosity, and is mass-produced.	1
2.	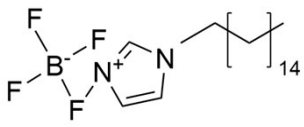	2D	ionic	1.4×10^{-3} S cm^{-1} at 30 °C	It combines the amphiphilic feature of imidazolium 1-hexadecyl-3-methylimidazolium tetrafluoroborate with propylene carbonate and $LiBF_4$, distinguishing it from other conventional electrolytes	It is classified as ionic LCEs, with potential applications in electrochemical devices (e.g., fuel cells, supercapacitors, and fluorination media).	2
3.	poly-(methoxy-poly (ethylene glycol) methacrylate)	2D	non-ionic polymer	1.0×10^{-7} S cm^{-1} at 25 °C	It has combined with LC or hydrophobic blocks to further improve its properties, setting it apart from other conventional polymer electrolytes.	It is a classical compound in the liquid crystal display (LCD) field, first commercialized in the 1970s by companies such as Merck & Co., Inc.	3
4.	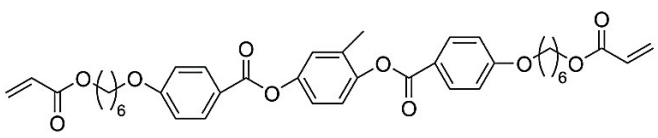	3D	non-ionic	1.79×10^{-3} cm^{-1} at 20 °C	It combines with ionic liquids (IL) to form polymer networks, which exhibits enhanced electrochemical properties compared to other electrolytes.	C6M is a custom-synthesized monomer that has not yet been commercialized on a large scale. Its high-purity synthesis is costly (estimated to be over $500 per gram), and it requires strict inert environment handling, which limits its industrial applications.	4

5.	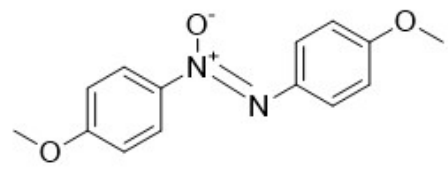	2D	non-ionic	1.3×10^{-4} S cm^{-1} at room temperature	It is a laboratory-grade innovative electrolyte, designed to address the interface compatibility and dendrite issues of SSBs. It has not yet been commercialized, but is described as a promising strategy.	5
6.	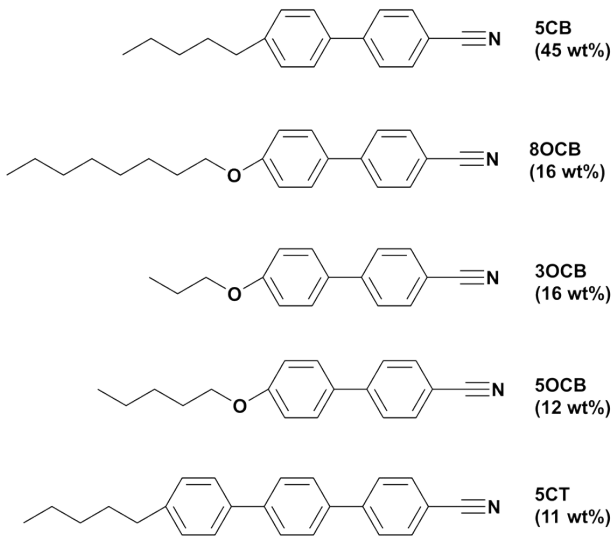	2D	non-ionic	10^{-6} S cm^{-1} at 72 °C	As a new type of solid electrolyte, it is targeted for applications in rechargeable metal ion batteries ($Li^{+}/Na^{+}/Mg^{2+}$), aiming to solve problems such as leakage of liquid electrolytes and dendrite growth.	6
7.	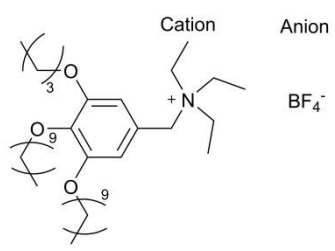	3D	ionic	-	It is a prototype compound developed in the laboratory and can be used as a candidate material for SSEs and fuel cells.	7
8.	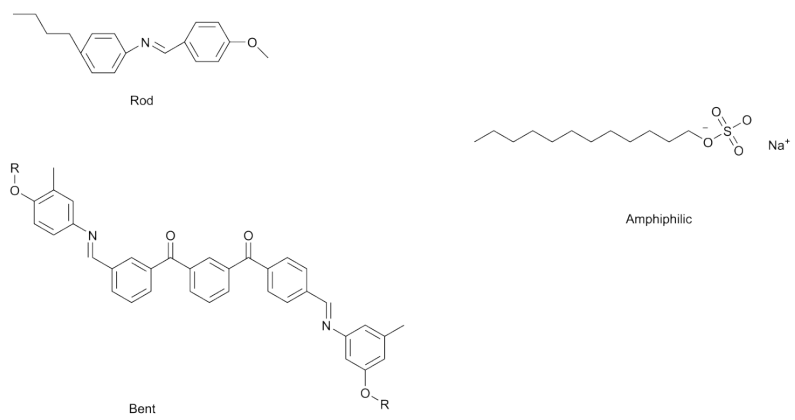	2D	ionic	-	The electro-optic effect of graphene oxide LCs is applied to optical switch devices, but has not yet been commercially utilized on a large scale.	8
9.	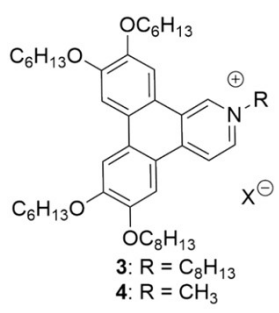	2D	ionic	-	There are no direct commercialization cases, but basic research has been active (since year 2010 to present), and the target applications include: organic semiconductors (photovoltaics, OLEDs, transistors), ionic conductive electrolytes (LIBs, fuel	9

							cells), and fluorescent sensors (anion-selective luminescence)	
10.	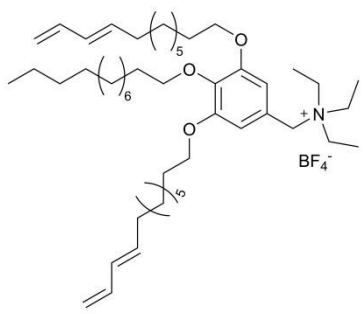	3D	ionic	3.1×10^{-4} S cm^{-1} at 90 °C , 7.75×10^{-5} S cm^{-1} at 90 °C, 8.8×10^{-6} S cm^{-1} at 90 °C		It is currently used in the laboratory research stage and has not yet been commercially scaled up. It applies potential as a new type of functional material in areas such as separation membranes, ionic conductors, and adsorbents.		10
11.	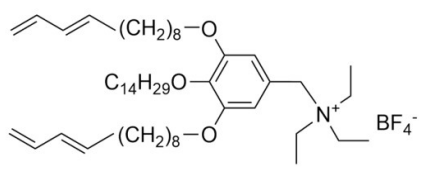	2D	ionic	-		It can be used for virus filtration and is a new material at the laboratory stage, with potential for industrial applications.		11
12.	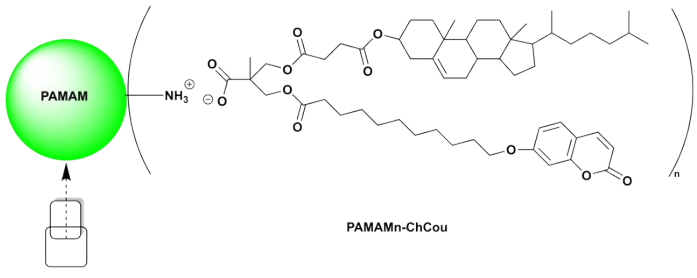	1D or 2D	ionic	$10^{-4} \sim 10^{-3}$ S cm^{-1} from 25 °C to 100 °C	The material uses ionic LC dendrimers to create tunable 1D/2D proton-conductive channels stabilized by coumarin photocrosslinking.	It is targeted at proton exchange membranes (PEMs) used in fuel cells and electrochemical devices, but it is currently still in the proof-of-concept stage.		12

Table S3 Performance summarization of LCEs

Number	Chemical Formula	Electrochemical stability	Thermal stability	Mechanical properties	Ease of fabrication	Interface compatibility	Safety	Cost	Scalability	ref.
1.	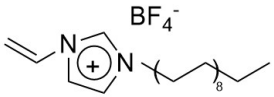	The electrochemical window is 5.2 V. It is superior to liquid electrolyte.	Decomposition temperature of inoic LC monomer: 268 °C. Meeting the safety requirements of lithium batteries (>200 °C), superior to flammable liquid electrolytes.	Self-supporting flexible membrane (free-standing and flexible), capable of bending, with a cross-linked structure (PEGDA photopolymerization) providing mechanical strength	One-pot photopolymerization (a mixture of ILC/PEGDA/PEGDE/$LiBF_4$ + UV curing)	Suppressing lithium dendrites, low interfacial resistance	The all-solid-state structure eliminates the risk of liquid leakage. No volatile solvents, high thermal stability.	High cost	Solution processing is conducive to scaling up.	13
2.	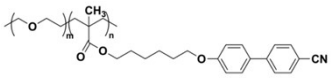	-	High decomposition temperature (290 °C), stable interlamellar ordered structure.	The star-shaped structure enhances flexibility, while the interlamellar units provide strength.	The film was prepared by atom transfer radical polymerization (ATRP) synthesis and induced to form a lamellar ordered structure	The hydrophilic poly-(methoxy poly (ethylene glycol) methacrylate) (PPEGMA) block promotes contact with the electrode, and the PEO side chain has a strong ability to dissolve lithium salts.	Fully solid-state intrinsically safe structure	High cost	The yield of star-shaped polymers is relatively low (requiring multiple purification steps), and there are challenges in large-scale productions.	3

					through liquid crystalline state annealing (at 95- 100 °C).					
3.	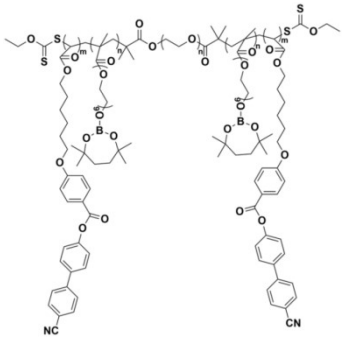	The electrochemical window is wide, measured at 4.85 V.	Decomposition temperature of 390 °C, with no leakage risk	Optimize the interface through the use of fluorinated ethylene carbonate (FEC) additives	Solution casting method is compatible with existing processes	Adding FEC to the lithium metal interface can inhibit the side reaction between the cyano-group and lithium.	The solid electrolyte is non-flammable and shows no thermal runaway during puncture/cutting tests.	High cost	-	14
4.	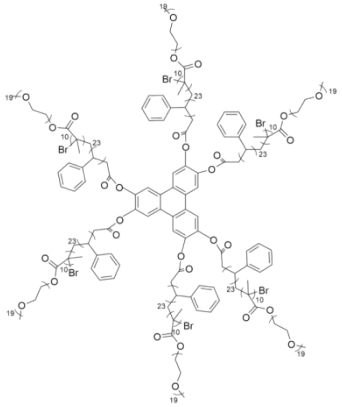	The electrochemical window is 5.1 V, meeting the requirement of high voltage.	Decomposition temperature of 390 °C, no leakage risk, superior to liquid electrolyte	It has a flexible self-supporting membrane that can restore its shape after being bent.	Solution casting (in THF) and annealing (at 120 °C) induce an ordered structure.	Low polarization, no dendrites	Fully solid-state, without risk of combustion or explosion	High cost	-	15
5.	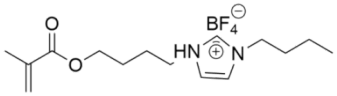	Electro-chemical window > 4.2 V, meeting the requirement of	The decomposition temperature is greater than	The composite electrolyte forms a self-	UV curing is fast and efficient.	The cyclic stability is good (> 85%), and the interface is	Non-flammable and no leakage	High cost	-	16

		high voltage.	290 °C. The ionic liquid characteristics eliminate the risk of volatile leakage of the traditional liquid electrolyte.	supporting film, with the cross-linking agent PEGDA providing the network framework, and the ordered structure of the LC phase enhancing the mechanical strength.		relatively stable.			
6.	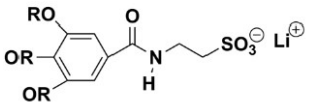 $R=CH_2=CHC(O)O(CH_2)_{11}$-	-	-	Self-supporting films possess the characteristics of flexibility, transparency and high mechanical strength.	-	-	Solid-state encapsulation of liquid electrolyte, eliminating the risks of leakage and combustion.	High cost	-	17
7.	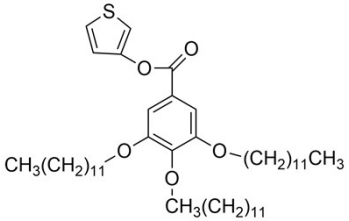	The electrochemical window is 4.0 V, meeting the requirement of high voltage.	Good thermal stability	-	Multi-step synthesis, solvent-assisted coating	-	Solvent-free design reduces the risk of explosion	High cost	-	18

8.	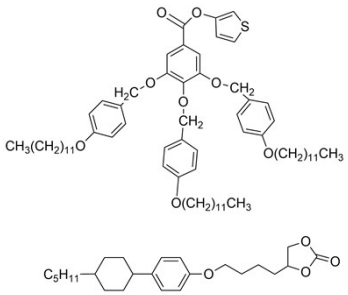	The electrochemical window is as wide as 3.9 V, and the cycling stability is excellent, thus meeting the requirements for high voltage applications.	This phase persists in a LC state within the temperature range from room temperature up to either 80 °C or 53 °C.	-	The solution processing approach is viable; however, precise control of components poses significant challenges.	The electrode interface exhibits good compatibility with both the Li metal anode and the $LiFePO_4$ cathode, characterized by a low interface impedance.	Minimize the risks of leakage and volatilization	High cost	-	19
9.	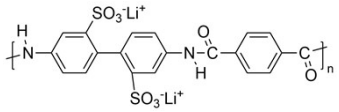	The electrochemical window measures 5.6 V.	The thermal stability is satisfactory. The LiFSI nanocrystals commence to degrade at 140 °C.	The mechanical properties far exceed those of traditional SPEs (typically < 10 MPa), approaching the rigidity of ceramic electrolytes, and can effectively prevent lithium dendrite penetration.	Two-step process: RMIC preparation and LiMIC preparation	The interface of lithium metal is capable of forming a stable solid electrolyte interphase (SEI) layer, and the corresponding interfacial impedance remains relatively low.	Without volatile solvents, it completely eliminates the risk of leakage and combustion.	High cost	-	20

10.	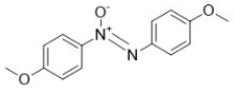	The electrochemical window is 4.9 V, meeting the requirement of high voltage.	-	The 3D fiber network structure enhances mechanical strength and effectively blocks dendrite penetration.	In-situ polymerization: A solvent-free approach (no solvent is necessitated). It involves the direct polymerization of the precursors (PEGDMA /ETFP/ LC) within the battery.	-	Solid-state structure, tested through bending and pricking methods	High cost	-
11.	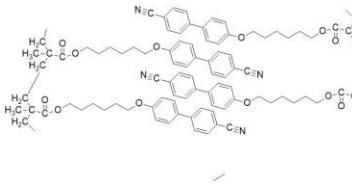	The electrochemical window is 4.5 V, meeting the high-voltage requirements.	It has good thermal stability. It does not shrink after being heated at 150 °C for 60 minutes. It begins to decompose at 350 °C.	PEGDA cross-linking provides the supporting framework, while the liquid crystal copolymer induces microphase separation.	Solution casting, UV curing, room temperature drying, vacuum annealing	-	It is flame-retardant and has no leakage risk.	High cost	-

12.	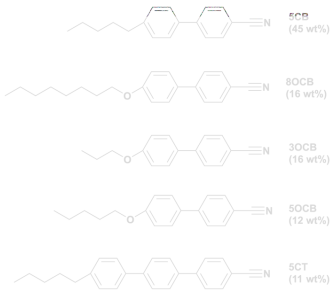	-	The thermal stability is poor and the melting point of the material is relatively low.	With self-supporting flexible membrane and capable of being bent and shaped.	Solution casting method	-	Solid-state system, no leakage, low flammability, inhibition of dendrite growth	Moderate to high costs	-	6
13.	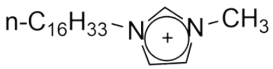 $^{-}PF_6$	Limited PF_6^- hydrolysis, with a relatively narrow voltage window.	The phase transition temperature is moderate (<125 °C)	Dependent on porous substrates, it is flexible but has limited strength.	Alumina film surface treatment (PVA/C16TAB) → Capillary filling (isotropic phase at 140 °C)	-	The PF_6^- anion will hydrolyze upon contact with water, generating HF (a highly toxic and corrosive substance), and a strictly dry environment is required.	High cost	-	22

14.		-	Excellent thermal stability	-	Solution-based film formation (THF solution spin coating) achieves uniform films	-	Low volatility but with the risk of fluorine-containing anions	High cost	-	9
15.	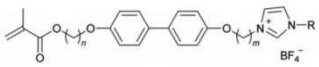	-	The operating temperature for water treatment is within the range of room temperature to 100 °C,but high-temperature applications are limited.	The ultrathin film (100 - 150 nm) is supported on a polysulfone substrate.	Photopolymerization (UV-LED) + Sacrificial Layer Transfer Method (PVA-coated PET film → Polysulfone substrate)	-	No leakage risk	High cost	The spin-coating and UV polymerization process have the potential for large-scale applications, but the large-scale production of ultra-thin and defect-free films remains to be verified.	23

16.	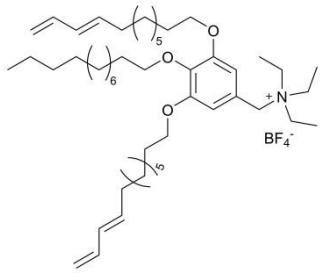	-	The polymer film remains stable up to 120 °C.	It has a self-supporting film that is insoluble in water and organic solvents, indicating that the cross-linked network is stable.	-	-	Fully solid-state, with no risk of solvent leakage	High cost	-
17.	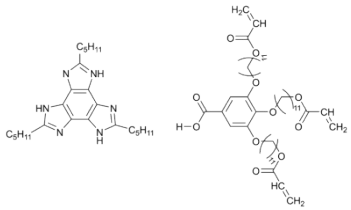	-	Forming a highly cross-linked LCNs through photopolymerization/thermal curing, enhancing stability	Introducing covalent "nanosticks" or increasing the crosslinking density can maintain the integrity of the pore channels.	Self-assembly reduces costs and is processable by solution method.	-	No heavy metals or volatile solvents. Theoretical safety is high.	High cost	-
18.	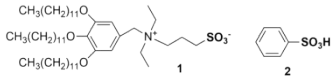	-	-	-	Solution casting and vacuum drying	-	The water-free system avoids the risk of high-temperature steam pressure. Benzenesulfonic acid is less corrosive	High cost	-

							than strong inorganic acids.			
19.		-	The phase transition temperature is relatively low.	After crosslinking, it forms polymer networks, enhancing mechanically stable	The PAMAM dendrimer macromolecules (G0-G4) and the coumarin-cholesterol dendrasylic acid (Ac-ChCou) self-assemble through ions. Solvent evaporates to form a film, followed by UV irradiation	-	UV curing without the use of initiators results in fewer side reactions and is relatively safer.	High cost	-	12

Reference

1. X. Wang, Z. He, R. Yan, H. Niu, W. He and Z. Miao, *Chemical Engineering Journal*, 2025, **503**.
2. H. Ruan, K. Lu, S. Meng, Q. Zhao, H. Ren, Y. Wu, C. Wang and S. Tan, *Small*, 2023, **20**.
3. Y. Tong, L. Chen, X. He and Y. Chen, *Journal of Power Sources*, 2014, **247**, 786-793.

4. M. Yao, H. Zhang, K. Dong, B. Li, C. Xing, M. Dang and S. Zhang, *Journal of Materials Chemistry A*, 2021, **9**, 6232-6241.
5. J. Li, F. Huo, Y. Yang, T. Chen, Y. Cui, Y. Cai and H. Zhang, *Chemical Engineering Journal*, 2022, **433**.
6. H. K. Koduru, Y. G. Marinov, G. B. Hadjichristov, A. G. Petrov, N. Godbert and N. Scaramuzza, *Journal of Non-Crystalline Solids*, 2018, **499**, 107-116.
7. A. E. Frise, T. Ichikawa, M. Yoshio, H. Ohno, S. V. Dvinskikh, T. Kato and I. Furó, *Chem. Commun.*, 2010, **46**, 728-730.
8. S. Padmajan Sasikala, J. Lim, I. H. Kim, H. J. Jung, T. Yun, T. H. Han and S. O. Kim, *Chemical Society Reviews*, 2018, **47**, 6013-6045.
9. K.-Q. Z. Jia Dai, Bi-Qin Wang, Ping Hu, Benoît Heinrich, Bertrand Donnio, *HAL*, 2020.
10. T. Ichikawa, M. Yoshio, A. Hamasaki, J. Kagimoto, H. Ohno and T. Kato, *J Am Chem Soc*, 2011, **133**, 2163-2169.
11. D. Kuo, M. Liu, K. R. S. Kumar, K. Hamaguchi, K. P. Gan, T. Sakamoto, T. Ogawa, R. Kato, N. Miyamoto, H. Nada, M. Kimura, M. Henmi, H. Katayama and T. Kato, *Small*, 2020, **16**.
12. A. Concellón, T. Liang, A. P. H. J. Schenning, J. L. Serrano, P. Romero and M. Marcos, *Journal of Materials Chemistry C*, 2018, **6**, 1000-1007.
13. S. Wang, X. Liu, A. Wang, Z. Wang, J. Chen, Q. Zeng, X. Wang and L. Zhang, *Polymer Chemistry*, 2018, **9**, 4674-4682.
14. Q. Zeng, Y. Liu, B. Wujieti, Z. Li, A. Chen, J. Guan, H. Wang, Y. Jiang, H. Zhou, W. Cui, S. Wang and L. Zhang, *Chemical Engineering Journal*, 2024, **486**.
15. S. Wang, A. Wang, C. Yang, R. Gao, X. Liu, J. Chen, Z. Wang, Q. Zeng, X. Liu, H. Zhou and L. Zhang, *Journal of Power Sources*, 2018, **395**, 137-147.
16. X. Chen, Y. Xie, Y. Ling, J. Zhao, Y. Xu, Y. Tong, S. Li and Y. Wang, *Materials & Design*, 2020, **192**.
17. R. L. Kerr, S. A. Miller, R. K. Shoemaker, B. J. Elliott and D. L. Gin, *J Am Chem Soc*, 2009, **131**, 15972-+.
18. K. A. Bogdanowicz, P. Gancarz, M. Filapek, D. Pociecha, M. Marzec, I. Chojnacka and A. Iwan, *Dalton Transactions*, 2018, **47**, 15714-15724.
19. T. Onuma, E. Hosono, M. Takenouchi, J. Sakuda, S. Kajiyama, M. Yoshio and T. Kato, *ACS Omega*, 2018, **3**, 159-166.
20. P. W. Majewski, M. Gopinadhan and C. O. Osuji, *Polymers*, 2019, **11**.
21. X. Cao, J. Cheng, X. Zhang, D. Zhou and Y. Tong, *International Journal of Electrochemical Science*, 2020, **15**, 677-695.
22. a. Y. Uchida, b T. Matsumoto,a T. Akitaa and N. Nishiyamaa, *Journal of Materials Chemistry C*, 2012, DOI: 10.1039/x0xx00000x.
23. T. Sakamoto, K. Asakura, N. Kang, R. Kato, M. Liu, T. Hayashi, H. Katayama and T. Kato, *Journal of Materials Chemistry A*, 2023, **11**, 22178-22186.
24. J. Lugger, D. Mulder, R. Sijbesma and A. Schenning, *Materials*, 2018, **11**.
25. B. Soberats, M. Yoshio, T. Ichikawa, S. Taguchi, H. Ohno and T. Kato, *J Am Chem Soc*, 2013, **135**, 15286-15289.